AIAA 2001-1214
High Temperature Polyimide Materials in Extreme Temperature Environments

T. F. Johnson and T. S. Gates
NASA Langley Research Center
Hampton, VA

42nd AIAA/ASME/ASCE/AHS/ASC Structures, Structural Dynamics and Materials Conference and Exhibit
16-19 April 2001 / Seattle, Washington

AIAA-2001-1214

HIGH TEMPERATURE POLYIMIDE MATERIALS IN EXTREME TEMPERATURE ENVIRONMENTS[1]

Theodore F. Johnson[+] and Thomas S. Gates*
NASA Langley Research Center, Hampton VA 23681

Abstract

At the end of the NASA High Speed Research (HSR) Program, NASA Langley Research Center (LaRC) began a program to screen the high-temperature Polymeric Composite Materials (PMCs) characterized by the HSR Durability Program for possible use in Reusable Launch Vehicles (RLVs) operating under extreme temperature conditions. The HSR Program focused on developing material-related technologies to enable a High Speed Civil Transport (HSCT) capable of operating temperatures ranging from 54°C (-65°F) to 177°C (350°F). A high-temperature polymeric resin, PETI-5 was used in the HSR Program to satisfy the requirements for performance and durability for a PMC. For RLVs, it was anticipated that this high temperature material would contribute to reducing the overall weight of a vehicle by eliminating or reducing the thermal protection required to protect the internal structural elements of the vehicle and increasing the structural strain limits. The tests were performed to determine temperature-dependent mechanical and physical properties of IM7/PETI-5 composite over a temperature range from cryogenic temperature -253°C (-423°F) to the material's maximum use temperature of 230°C (450°F). This paper presents results from the test program for the temperature-dependent mechanical and physical properties of IM7/PETI-5 composite in the temperature range from -253°C (-423°F) to 27°C (80°F).

Introduction

The NASA Reusable Launch Vehicle (RLV) Program was initiated in 1994 [1]. The goal of the RLV Program was to develop launch vehicles that would have aircraft-like operation. The products to be developed from the program were new structural systems and materials that decreased the cost per pound of launching a payload to orbit, reduced risk, and decreased vehicle turnaround time for the subsequent launch. The RLV Program planners used the NASA Access to Space Study to establish baseline architecture and anticipated benefits for key known and emerging technology, Figure 1 [2]. The results of the study suggested that a series of experimental scaled RLV X-vehicles (X-33, X-34) should be built using current and emerging technology to demonstrate that key technological obstacles could be overcome [3].

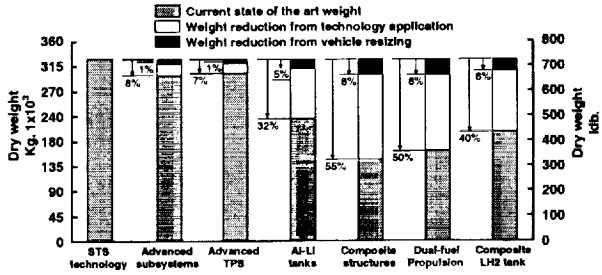

Figure 1. Predicted weight reduction and vehicle resizing from the incorporation of advanced technology [2].

One of the most challenging obstacles for the RLV Program was development of the reusable integral cryogenic propellant tanks. Internal cryogenic tanks comprise 35 percent of the dry weight of the vehicle and occupy most of the internal volume as seen in Figure 2 [3]. Launch vehicles are typically weight critical and, as shown in Figure 1, development of Polymeric Matrix Composite (PMCs) LH_2 tanks offer significant benefits. If the tanks of an RLV were to be constructed of PMCs, the prevention of permeation of hydrogen (H_2) through the tank wall membrane would be a major technical challenge.

The TPS weight can rival the weight of the primary structure. In itself, advances in TPS technology do not yield impressive performance gains (See Figure 1), however, increasing the temperature limit of the material being protected can directly affect TPS weight. Benefits of high temperature PMC materials as compared to lower temperature PMC's become evident when the tank is designed as an

+ Aerospace Engineer, Metals and Thermal Structures Branch.
* Senior Materials Research Engineer, Mechanics and Durability Branch, Associate Fellow, AIAA.

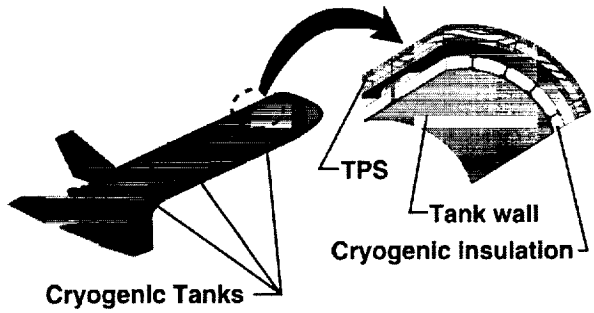

Figure 2. Generic Reusable Launch Vehicle (RLV), with internal cryogenic propellant tanks and cross-section of an integrated cryogenic propellant tank.

integrated system consisting of the tank wall, cryogenic insulation and Thermal Protection System (TPS), Figure 2 [4,5]. The limiting factors in reducing the TPS thickness and weight have been the reusable cryogenic foam and the tank wall. If advanced high temperature reusable cryogenic insulation foams that can operate at temperatures of 177°C (350°F) or higher [6] are employed, then the maximum temperature of the PMC tank wall controls the TPS sizing. A higher temperature polyimide PMC tank wall would enable the reduction of the TPS thickness and weight, reducing the overall weight of the vehicle.

The NASA High Speed Research (HSR) Program developed advanced material concepts for application in the High Speed Civil Transport (HSCT) [7]. This commercial aircraft was designed to fly at speeds of Mach 2.4 and carry up to 300 passengers. The materials used in the vehicle had to be durable enough to retain design strength and stiffness levels over 60,000 hours of operation at temperatures up to 177°C (350°F). Materials from the HSR Program potentially could be used in an RLV to reduce structural weight because of the material's ability to be used at higher operating temperatures and at high strain levels for a short period of time. An experimental program was developed to investigate the mechanical and physical properties of HSR materials at the extreme operational temperatures of an RLV. This paper will discuss the results obtained from for the polyimide material IM7/PETI-5 in the temperature range from -270°C (-452°F) to 27°C (80°F), representing the lower temperature extremes typical for cryogenic propellant tanks.

Material

The PMC material used in this study, IM7/PETI-5, consisted of a high strength, intermediate modulus carbon fiber in a thermoplastic polyimide matrix. All tests were performed on laminated composites fabricated at the Northrop Grumman Corporation (NGC), Dallas, TX. These composite panels consisted of three basic lay-ups: $[0]_8$, $[0]_{13}$, $[\pm 45]_{3S}$, and a unique 13 ply layup that was designated as RLV orthotropic. The $[45/90_3/-45/0_3/-45/90_3/45]$ layup was designated RLV [0] and the layup $[-45/0_3/45/90_3/45/0_3/-45]$ was designated RLV [90]. These orthotropic layups were chosen to be representative of a composite wall in a typical cryogenic propellant tank. The RLV [0] designation represented orientation of the 0° ply in the longitudinal axis direction of the vehicle, while the RLV [90] designation represented orientation of the 0° ply in the circumferential or hoop direction of the tank.

All panels were fabricated by hand lay-up, and after every other ply a five minute room temperature vacuum compaction was performed throughout the entire process. The bagging and cure processes employed were consistent with standard practices. The cure cycle consisted of a 240 (+/-10) minute hold at 177°C (350°F), a 120 (+/-10) minute hold at 260°C (500°F) under full vacuum, followed by pressurization of the autoclave to 1480 (+/-35) kPa [200 (+/-5)] psig at 170 (+/- 14) kPa/minute [10 (+/-2) psig/minute] during ramp to 370°C (700°F) for 60 (+/-10) minute. Through-transmission, ultrasonic inspection indicated that there were no significant internal anomalies in any of the panels.

Test Methods and Procedures

All of the material tests reported here were focused on screening the material IM7/PETI-5 for cryogenic tank application. The Boeing Corporation, Huntington Beach, CA with Materials Research & Engineering (MRE) in Boulder, CO conducted a majority of tests in this program. Mechanical and physical properties were determined at room temperature for a baseline and at liquid nitrogen (LN_2) -195°C (-320°F) temperatures and when possible at liquid helium (LHe) -270°C (-452°F) temperatures. In most cases, a minimum of 3 replicates were used for any test condition. A portion of the material samples were thermally cycled from cryogenic temperatures -253°C (-423°F) to 205°C (400°F) in an unloaded state to investigate the aging effects of thermal cycling.

The material property test program investigated temperature effects on unaged, as-received materials for unnotched tension, notched tension, compression, in-plane shear, and Coefficient of Thermal Expansion (CTE), as shown in Table 1. The open-hole notched versus unnotched tests determined whether a flaw or bolthole would significantly decrease the mechanical properties of the material. In a cryogenic tank design, however, the number of penetration point or open holes is minimized and different design criteria may be required to develop a damage tolerance design. The temperature dependent physical properties investigated were density, thermal conductivity, oxygen compatibility, and permeability, Table 1. The CTE data supports the thermal-mechanical stress analysis of the laminate using classical lamination theory and can be used in design to develop configurations that minimize microcracking.

Table 1. Test Matrix for PMCs.

Test Type	Unidir. 0°, 90°	$[\pm 45]_{3s}$	RLV Orthotropic [0], [90]	
			Not Cycled	Therm. Cycled
UNT stiffness	X, X	X	X, X	X, X
UNT strength	X, X	-	X, X	X, X
UNC stiffness	X, X	X	X, X	X, X
UNC strength	-	-	X, X	X, X
NTS	-	-	X, X	X, X
CTE	X, X	-	X, X	-
Thermal conduct.	X, NA	-	-	-
Density	X, NA	-	-	-
H_2 Perm.	-	-	X	X
LOx Compat.	-	-	X	-

Notes:
Minimum number of replicates = 3 (where applicable)
UNT = Unnotched tension (ASTM D3039) (ASTM D3518-76 for in-plane shear $[\pm 45]_{3s}$)
UNC = Unnotched compression (ASTM D3410-87)
NTS = Notched tensile strength (SACMA SRM 5-88)
CTE = Coefficient of Thermal Expansion (ASTM C177)

Mechanical Property Tests

All of the mechanical property tests were considered quasi-static and were conducted using standard test methods. The appropriate ASTM or SACMA test standard for each test type is noted in Table 1. Modulus was calculated according to the procedures provided in the test specification. Ultimate strength was defined as the point in the test profile where a complete loss of load carrying capability was observed.

The notched and unnotched tension tests were performed on 98-N (22-Kip) and 245-N (55-Kip) computer controlled, hydraulic test frames. A cross-head speed of 1.3 mm/min. (0.05 in./min.) was utilized for all tension tests. The compression tests were performed on an 89-N (20-Kip), electro-mechanical test frame. A cross-head speed of 1.3 mm/min. (0.05-in./min.) was utilized for all compression tests. Load as measured by the load cell, stroke as measured by the test machine displacement transducer, and strain as measured via strain gages and standard instrumentation were recorded for each test. Strains were recorded using Measurements Group's* WK-06-125AD-350 gages with an operational temperature range of -270°C (-452°F) to 290°C (550°F).

The unnotched tension and compression strength specimens required end tabs. Tabbing materials and adhesives for the bonding of specimen varied depending on the environmental test condition. The tabs for the tension specimens tested below 177°C (350°F) were made from E-glass/Bismaleimide (BMI) and bonded with Cytecfiberite FM-300 film adhesive.

Thermal cycling

Thermal cycling was conducted in the Thermal Structures Laboratory at LaRC on unloaded IM7/PETI-5 panels to investigate the effects of cyclic temperature change on the material's residual notched and unnotched strength and stiffness, and permeation after thirty-five thermal cycles. The specimens were machined from the panels after thermal cycling to avoid edge effects such as delamination effects from thermal cycling. The permeation specimens were premachined prior thermal cycling to meet test schedule. Panels and specimens were placed in stainless steel baskets that were subjected to different temperature environments at four stations for 20 minute intervals. The four stations were cryogenic temperatures (LN_2 or LHe), warming in ambient air, high temperature oven (205°C [400°F]) and cool down in ambient air. Before a basket was placed in LHe, the basket and its contents were pre-chilled in LN_2. Cycle 1 ranged in temperature from -270°C (-452°F) to 205°C (400°F), while Cycle 2 ranged in temperature from -160°C (-320°F) to 205°C (400°F).

Coefficient Thermal Expansion (CTE) Tests

The CTE measurements were made in accordance to ASTM E228 over a temperature range of -253°C (-423°F) to 227°C (440°F) using a 1.0 cm (0.4 in.) to 1.5 cm (0.6 in.) long specimen. A calibrated thermocouple was placed 2.5 mm (0.1 in.) away from the specimen and the specimen was uniformly heated at a constant rate of < 3K/min. The thermal expansion of the specimen was measured with a vitreous push rod and a Linear Voltage Displacement Transducer (LVDT). The CTE was determined from the thermal expansion data using the instantaneous slope method at the completion of the test.

Thermal Conductivity Tests

The through-the-thickness thermal conductivity was measured at three temperatures -268°C (-450°F), -195°C (-320°F), and 27°C (80°F). The tests were performed using a test standard similar to ASTM C177. Individual test specimens were placed in the thermal conductivity apparatus in contact with hot and cold plates, and the apparatus was inserted into a temperature-controlled chamber. Thermal conductivity tests were performed by maintaining a fixed cold plate temperature using LHe or LN_2 and monitoring the

*This is not an endorsement by the National Aeronautics and Space Administration (NASA)).

power required to maintain a hot plate under steady state conditions.

Permeation Tests

All of the tests described thus far have been standard material characterization tests except for the temperature aspects. Cryogenic tanks, however, have criterion that requires application specific tests to determine a material's feasibility. The H_2 permeation tests determine a materials ability to contain H_2 at various temperatures [8]. The bench top permeability tests were conducted at Boeing-Huntington Beach, CA using 4.76-4.92 cm (1.875-1.9375 in.) diameter flat disks. The specimen was not under a mechanical load when tested but a vacuum was drawn on the H_2 detection side while pressurized gaseous hydrogen (GH_2) was introduced to the opposite side. If the test was at cryogenic temperatures, the entire test coupon holder was cooled using LN_2 for one hour before the test. Once the specimen was at the target temperature, GH_2 was introduced into the GH_2 chamber at a pressure of 445 kPa (50 psig) for 16 hours to absorb GH_2 and reach a steady state of diffusion or leak. A residual gas analyzer (RGA) measured the amount of H_2 that penetrated the specimen.

LOx Compatibility Tests

NASA Marshall Space Flight Center (MSFC) conducted the LOx compatibility tests in the Materials Combustibility Research Facility. The test simulated the reaction that occurs when two materials collide at various impact energies in a pure oxygen environment at various temperatures and pressures. In the tests at MSFC [9], a 1.3 cm (0.5 in.) square of a candidate material was placed in an aluminum or stainless-steel cup, which was then filled with liquid or gaseous oxygen. The pressure and temperature were adjusted to simulate the specified conditions. A striker pin was placed in contact with the sample and was then impacted with a 9 Kg (20 lbs.) plummet, which, in combination with the drop-height, produced an impact energy of 10 Kg-m (72 ft-lbs.). If the material reacted when impacted, the impact energy was reduced. Twenty samples of the material were impacted and any reaction was noted. A reaction consisted of an audible report, a flash, or evidence of burning. No reaction out of twenty impacts indicated that a material was acceptable for use in the tested oxygen environment. Two or more reactions constituted failure of the sample and indicated that the material was not acceptable for use in the tested oxygen environment. If one reaction out of twenty impacts occurred, the material had to survive forty additional impacts to be acceptable.

Results

The results of all the tests discussed in this section are referenced to the corresponding figures and tables. In terms of performance, the primary independent variables considered are test temperature and specimen layup.

Strength and Stiffness

The effects of temperature change on the mechanical properties of strength and modulus were investigated for unidirectional laminates at ambient, LN_2 (-195°C [-320°F]) and LHe (-270°C [-452°F]) temperatures. Table 2 contains the numerical averages for all of the mechanical property tests. The decrease in temperature did not effect the tension strength of the 0° unidirectional laminate but did increase the compression strength, Figure 3. In a similar manner, the tension and compression strengths of the 90° unidirectional laminate increased as temperature decreased, Figure 4. Temperature had a moderate effect on tension and a larger effect on compression.

The tension and compression moduli for the 0° unidirectional laminate were not significantly affected by temperature but the tension modulus slightly increased at the lowest test temperature, Figure 5. Lowering the test temperature for the 90° unidirectional laminate moderately increased the tension and compression moduli, Figure 6. The in-plane shear modulus was also determined at temperatures ranging from -252°C (-423°F) to room temperature using $[\pm 45]_{3S}$ laminates. The in-plane shear modulus increased as the temperature decreased, Figure 7.

The RLV orthotropic laminate mechanical properties of unnotched strength and modulus, notched strength were investigated for temperature and thermal cycling effects. The test temperature decrease affected both the RLV [0] and RLV [90] laminates by increasing strength, Figures 8 and 9. The RLV [90] displayed a greater sensitivity to temperature than the RLV [0] laminate. Both orientations had a large separation between tension and compression strength over the temperature range plotted but both converged at the lowest test temperature. The tension and compression moduli for both the RLV [0] and [90] laminates plotted in Figures 10 and 11 respectively were not significantly affected by temperature. There was however, a separation between the tension and compression values.

Notch sensitivity of the RLV laminates in tension was investigated as a function of test temperature. In comparison to the unnotched tension strength, notches significantly reduced the strength by fifty percent in a uniform fashion for both the RLV [0] and [90] laminates over the tested temperature range, Figures 12 and 13.

Table 2. Averaged mechanical modulus and strength test results for IM7/PETI-5.

Laminate, Orientation and Property Test	Value (Unit)	Test Temperature (°F)					
		-423	-320	75	350	400	450
Unidir. 0° UNT	Modulus (msi)	25.6	23.6	24.6	25.7	25.8	26.5
	UTS (ksi)	277.7	274.5	277.5	252.4	273.7	297.5
Unidir. 90° UNT	Modulus (msi)	1.9	1.7	1.6	1.3	1.3	1.2
	UTS (ksi)	8.7	11.3	6.1	5.1	4.1	3.2
Unidir. 0° UNC	Modulus (msi)	18.4	18.3	18.2	17.5	18.0	19.4
	UCS (ksi)	189.6	147.3	183.5	119.7	89.2	49.3
Unidir. 90° UNC	Modulus (msi)	1.8	1.8	1.4	1.1	1.0	0.8
	UCS (ksi)	57.7	55.2	37.8	-	16.1	17.5
In-Plane Shear UNC	Modulus (msi)	0.9	0.9	0.9	0.6	-	0.6
RLV [0] UNT	Modulus (msi)	8.5	8.6	8.2	10.2	9.4	9.7
	UTS (ksi)	111.9	115.6	108.4	109.3	111.4	107.7
RLV [90] UNT	Modulus (msi)	14.4	14.1	13	17.2	-	14.4
	UTS (ksi)	171.3	164.6	180.8	179.8	-	157.9
RLV [0] NTS	UTS (ksi)	53.2	50.7	49.4	55.7	54.1	53.1
RLV [90] NTS	UTS (ksi)	83.6	85.6	78.2	82.8	85.4	87.4
RLV [0] UNC	Modulus (msi)	6.5	6.2	6.6	5.7	4.7	5.1
	UCS (ksi)	110	97.2	80.6	72.3	64.1	45.2
RLV [90] UNC	Modulus (msi)	10.7	10.4	9.9	9.5	9.6	9.5
	UCS (ksi)	176.1	82.9	121.2	87.4	76.4	59.3

Note:
UNT = Unnotched tension UNC = Unnotched compression NTS = Notched tensile strength
UTS = Ultimate tension strength UCS = Ultimate compression strength

Thermal Cycling

The limited exposure or aging effects due to thermal cycling was investigated. After the material was thermally cycled thirty-five times, the specimens were tested at room temperature. Table 3 and the bar graphs in Figures 14 and 15 show that as the low end of the cyclic temperature was decreased, the material's residual strength for both the RLV [0] and [90] laminates decreased. The tension modulus was also affected in the same manner but to a lesser extent as shown in Figure 16.

For notched specimens only, the aging effects of thermal cycling and testing at room temperature on strength were compared to the strength of unaged specimens tested at temperature (Figures 17 and 18). The notched strength values from these two different test scenarios do not vary significantly.

Coefficient of Thermal Expansion (CTE)

The CTE of the 90° unidirectional laminate was an order of magnitude greater than the CTE of the 0° unidirectional laminate and was nonlinear with respect to temperature (Table 4, Figure 19). As the temperature decreased from 27°C (80°F) to -253°C (-423°F), the CTE of the 0° unidirectional and RLV [0] laminates increased. The CTE of the RLV [0] laminate was relatively flat in the temperature range between 27°C (80°F) to -253°C (-423°F) but had a slight increase in the intermediate temperatures.

Table 3. Averaged cycled RLV mechanical modulus and strength test results for IM7/PETI-5.

Orientation and Property Test	Value (Unit)	Low End Cycle Temperature	
		-423°F	-320°F
[0] UNT	Modulus (msi)	7.5	7.6
	UTS (ksi)	104.1	109.5
[90] UNT	Modulus (msi)	11.9	12.2
	UTS (ksi)	129.9	172.5
[0] UNC	UCS (ksi)	50.6	72.4
[90] UNC	UCS (ksi)	75.5	78.9
[0] NTS	UTS (ksi)	55.4	55.2
[90] NTS	UTS (ksi)	88.4	78

Notes:
UNT = Unnotched tension UNC = Unnotched compression
NTS = Notched tensile strength UTS = Ultimate tension strength
UTS = Ultimate compression strength

Table 4. Averaged Coefficient of Thermal Expansion (CTE) for IM7/PETI-5.

Test Temp. °C (°F)		Coefficient of Thermal Expansion μ in./in.-°F			
		Unidir. 0°-Dir.	Unidir. 90°-Dir.	RLV [0]	RLV [90]
27	(80)	-0.48	25.47	2.53	0.40
-73	(-100)	-0.02	21.73	2.69	0.66
-173	(-280)	0.84	16.87	2.81	1.39
-273	(-423)	1.55	8.69	2.53	1.67

Physical Properties

The density of the IM7/PETI-5 was 1.572 g/cm^3 (0.0568 lb/in.^{3}) at ambient conditions. The through-the-thickness thermal conductivity values in Table 5 precipitously decreased as the temperatures decreased, Figure 19.

Table 5. Thermal conductivity of IM7/PETI-5.

Temperature K (°F)		Thermal Conductivity w/mK
300	(80)	0.977
77	(-320)	0.764
5	(-452)	0.049

Permeability

All of the IM7/PETI-5 disks had a permeation rate less than the threshold of 8.50x10E-5 STD cc-mm/atm-sec.-cm^2 for containing H_2 in Table 6. Any permeation rate value greater than 8.50x10E-5 STD cc-mm/atm-sec.-cm^2 was not acceptable for use as a cryogenic LH_2 tank wall. There was an increase in permeability between the cycled and the uncycled specimens tested at room temperature and at -195°C (-320°F). The cycled and the uncycled disks tested at -195°C (-320°F) had a higher rate of permeability than both of the cycled and the uncycled disks tested at room temperature. The cycled disk tested at -195°C (-320°F) had the highest permeability rate.

Lox Compatibility

The LOx compatibility test results in Table 7 show that IM7/PETI-5 at 100 kPa (14.6 psia), -183°C (-300°F) in LOx passed only the lowest impact load of 1.4 Kg-m (10 ft-lbs.). The specimen tested at 345 kPa (50 psia), -183°C (-300°F) in LOx passed the maximum impact load of 10 Kg-m (72 ft-lbs.). The specimens tested with GOx at 345 kPa (50 psia), at temperatures of 24°C (75°F) and 205°C (400°F) failed at the maximum impact load of 10 Kg-m (72 ft-lbs.) but passed at the intermediate impact of load of 5.6 Kg-m (40 ft-lbs.).

Table 6. Permeability test results for IM7/PETI-5.

Thermally Cycled	Test Temp. °C (°F)		Permeation* STD cc-mm / atm-sec.-cm^2
None	24	(75)	1.14x10E-8
35 Times	24	(75)	1.98x10E-8
None	-195	(-320)	3.59x10E-8
35 Times	-195	(-320)	2.76x10E-7

* Pressure = 445 kPa (50 psig).

Table 7. LOx and GOx compatibility test results for IM7/PETI-5.

Test Conditions °C, kPa (°F, psia)	Impact Energy* Kg-m (Ft-lbs.)				
	10 (72)	6.9 (50)	5.6 (40)	3.5 (25)	1.4 (10)
LOx: 100, -183 (14.6, -300)	2/20	N/C	N/C	2/34	0/20
LOx: 345, -183 (50, -300)	0/20	N/C	N/C	N/C	N/C
GOx: 345, 24 (50, 75)	2/2	2/2	0/20	N/C	N/C
GOx: 345, 205 (50, 400)	2/4	2/4	0/20	N/C	N/C

*Values - No. reactions/No. impacts, ## = Failed
Note:
N/C - Not conducted

Discussion and Remarks

The matrix-dominated properties of the IM7/PETI-5 material were the properties most sensitive to decreases in test temperature. In general, transverse (90° unidirectional and RLV [0]) and in-plane shear stiffness increased as temperature decreased in Figures 6, 10, and 7. The increase in tension stiffness of the 0° unidirectional laminate as the temperature decreased may be attributed to an increase in matrix modulus. The small differences in modulus for tension and compression of the 90° unidirectional laminate over the complete temperature range were a good indication of the load direction insensitivity of this test method. The load direction insensitivity resulted from the fibers not contributing to the stiffness of the 90° unidirectional laminate. The increase in the modulus was solely produced from matrix stiffening as the temperature decreased. Both directions of the RLV laminates exhibited low sensitivity of modulus to test temperature although in general both laminates increased in stiffness as temperature decreased. Clearly, even laminates that approach a quasi-isotropic layup should increase in stiffness as the temperature decreases.

The results of the IM7/PETI-5 unidirectional laminates in Table 2 when compared to the toughened graphite-epoxy IM7/977-2 averaged values in Table 8

Table 8. Averaged IM7/977-2 mechanical modulus and strength from industry.

Laminate, Orientation and Property Test	Value (Unit)	General Dynamics Data Test Temperature (°F)				Rockwell Data Test Temperature (°F)		
		-423	-320	75	250	-423	75	190
Unidir. 0° UNT	Modulus (msi)	23.37	22.05	24.6	22.7	20.4	21.5	21.5
	UTS (ksi)	322	357	358	376	210	247	222.3
Unidir. 90° UNT	Modulus (msi)	-	-	-	1.22	2.81	1.35	1.08
	UTS (ksi)	-	-	-	9.1	12.65	8.1	7.20
Unidir. 0° UNC	Modulus (msi)	21.5	23.0	22.1	-	-	-	-
	UCS (ksi)	260.3	280.6	197.7	-	222	205	176.3
Unidir. 90° UNC	Modulus (msi)	-	-	-	-	-	-	-
	UCS (ksi)	-	-	-	-	36.53	40.5	36.0
In-Plane Shear UNT	Modulus (msi)	1.12	0.938	0.696	-	1.16	0.750	0.60
	UCS (ksi)	20.8	18.8	18.0	-	16.0	12.25	10.9

Notes:
UNT = Unnotched tension
UTS = Ultimate tension strength
UNC = Unnotched compression
UCS = Ultimate compression strength

obtained from various industry sources show that the IM7/PETI-5 material has comparable tension and strengths at the lower temperatures and superior strength and moduli at the elevated temperature. The IM7/977-2 has a higher compression moduli and strength and in-plane shear. than the IM7/PETI-5 material, however, IM7/PETI-5 also has greater transverse tension moduli and the strength does not roll-off as fast as the IM7/977-2 at the elevated temperatures.

Unnotched tension strength of the RLV [0] layup was not affected by decreasing temperature due to the dominance of the temperature insensitive fibers. Decreasing the temperature did affect the unnotched compression strength due to matrix stiffening at the lower temperatures that led to higher compression stability by suppressing microbuckling of fibers. This stiffening of the matrix and its effect on compression strength was also evident in the RLV [90] layup compression strength test results.

There was a roll-off in compression strength at the lowest temperature for the 90° unidirectional laminate. This can be attributed to the trade off between competing effects from stiffness and increases in brittleness. In general, the failure mode for tension loading was associated with splitting or breaks at the fiber to matrix interfaces while the failure mode for compression loading was associated with loss in stability resulting in localized buckling. Wide separation in unnotched strength values between tension and compression for both 0° and 90° unidirectional laminates can be attributed to the difference in failure modes.

These failure mode differences between tension and compression were also reflected in the strength of the RLV laminates at room temperature and -195°C (-320°F). Interestingly though, both the RLV [90] and RLV [0] laminates had a similar convergence of tension and compression strength at -253°C (-423°F). The almost quasi-isotropic layup yielded a smaller separation between tension and compression strengths. The lack of loading mode sensitivity at this temperature was significant and would imply the need to thoroughly explore the complete temperature range to establish clear trends.

Without a quantitative assessment of possible damage induced by thermal cycling, it was unclear if the decrease in stiffness and strength of the RLV laminates as shown by Figures 14-16 was strictly due to material property changes or property changes in conjunction with damage accumulation. It would be expected that if damage in the form of microcracks were to be present, then both strength and stiffness would decrease with an increase in damage. Assuming that the damage was caused by high strains associated with residual thermal stresses, then the thermal cycle with the largest temperature differential would induce the most damage.

Clearly, the stress concentrations due to the large center hole dominated the strength of the noncycled and thermally cycled notched specimens reducing the strength by fifty percent. The center hole notched specimens were also insensitive to temperature as seen in Figures 12 and 13. This was true regardless of whether the material had been thermally cycled and tested at room temperature or tested at temperature as evidenced by Figures 17 and 18. These results and figures indicated that the notched specimens were not appropriate for assessment of material property sensitivity to temperature.

The exposure to the high temperature of 205°C (400°F) during thermal cycling possibly contributed to

the degradation of the material properties tabulated in Table 3. In Table 2, the quasi-static results at 177°C (350°F) and 205°C (400°F) indicated that there was not a significant reduction in tension moduli and strength in the fiber-dominated 0° unidirectional and RLV [90] laminates. The tension moduli and strength for the matrix-dominated unidirectional 90° and RLV [0] laminates were affected by the increase in temperature as well as the in-plane shear modulus. There was however, a significant reduction in the compression moduli and strength of all laminates at the elevated temperatures. Fiber instability and elevated temperature sensivity of the matrix material possibly caused this reduction for the mechanical property tests at the elevated temperatures, and may have also affected the properties for the thermally cycled specimens.

The CTEs of the unidirectional laminate in the 0° direction, and the RLV [90] laminate increased as the temperature decreased from ambient to cryogenic temperatures, Figure 19. The CTE of the RLV [0] laminate remained relatively flat over the same temperature range. The CTE of the unidirectional laminate in the 90° direction, however, was nonlinear with respect to temperature. This nonlinearity can be attributed to the dominance of the matrix in the 90° unidirectional laminate versus the dominance of the fibers in the 0° unidirectional laminate. The matrix dominance in the RLV [0] laminate caused the CTE of the laminate to remain relatively flat in the cryogenic temperature range, while fiber dominance caused the CTEs of the 0° unidirectional and RLV [90] laminates to increased as the temperature decreased.

The thermal conductivity decreased with temperature in Figure 19 indicating that IM7/PETI-5 becomes a better insulator at cryogenic temperatures.

The H_2 permeation rate was acceptable for an LH_2 cryogenic tank wall. The reduction in test temperature increased the permeation rate significantly. Thermally cycling also degraded the materials ability to contain H_2 by increasing the permeation rate. A more conclusive test to determine a material's ability to contain LH_2 could be conducted if the material was under load or had been subjected to thermal/mechanical cyclic loading to simulate end of life aging prior to permeation testing.

The LOx compatibility test results, Table 7, indicate that the IM7/PETI-5 did poorly in a LOx rich environment. The samples tested in LOx at ambient pressure failed but passed the high pressure LOx test. The samples also marginally passed the GOx tests but did not qualify for LOx tank application. Free edge effects might have played a role in the material not passing the test at MSFC. The specimens were square in shape while standard metallic specimens were round. The square shape facilitated in the fabrication of the specimen and attempted to minimize frayed edges. An alternate LOx compatibility qualification test at NASA White Sands Tests Facility (WSTF) does not allow free edges to be in the impact region and allows the sample to flex when impacted, dissipating a portion of the impact energy [10]. A LOx compatibility test should be conducted using the techniques of WSTF in the future to determine if free edge effects played a role in the IM7/PETI-5 LOx compatibility results.

Summary and Conclusions

The results presented in this paper indicate that IM7/PETI-5 is a viable candidate for use as a LH_2 cryogenic tank material and primary structure for an RLV. The high use temperature of IM7/PETI-5 will reduce the TPS weight and the weight of the vehicle. The material exhibits temperature trends similar to IM7/977-2, has strengths that are of the same magnitude as IM7/977-2, and has passed the screening test for H_2 permeation suggesting that IM7/PETI-5 may be suitable for LH_2 tanks. Additional mechanical tests at intermediate temperature and with more replicates are required to verify temperature trends and reduce statistical error. Establishing strain limits, fracture toughness, thermal/mechanical aging effects, hydrogen permeability under load, and LOx compatibility at an alternate facility will solidify the suitability of IM7/PETI-5 for RLV LH_2 and LOx cryogenic propellant tank application in the future.

References

1. Cook, S., "The X-33 Advanced Technology Demonstrator," Presented at the American Institute of Aeronautics and Astronautics (AIAA) Dynamics Specialists Conference, AIAA-96-1195, April 1996.
2. NASA, "Access to Space Study Final Report," NASA Headquarters, Washington DC, July 1993.
3. Freeman, Jr., D. C., Stanley, D. O., Camarda, C. J., Lepsch, R. A., Cook, S. A., "Single-Stage-To-Orbit A Step Closer," Presented at the 45th Congress of the International Astronautical Federation (IAF), IAF 94-V3.534, October 1994.
4. Johnson, T. F., Natividad, R., Rivers, H. K., Smith, R., "Thermal Structures Technology Development for Reusable Launch Vehicle Cryogenic Propellant Tanks," Presented at the Space Technologies and Application International Forum, Albuquerque, NM, January 1998.
5. Myers, D. E. Martin, C. J., Blosser, M. L., "Parametric Weight Comparison of Advanced Metallic, Ceramic Tile, and Ceramic Blanket Thermal Protection Systems (TPS)," NASA Technical Memorandum L-17651, August 1997.
6. Weiser, E. S., Johnson, T. F., St. Clair, T. L., Echigo, Y., Kaneshiro, H., Grimsley, B.W., "Polyimide Foams for Aerospace Vehicles", Journal of High Performance Polyimides, Volume 12 (2000), pp. 1-12.
7. Committee on High Speed Research, National Research Council, "U.S. Supersonic Commercial

Aircraft - Assessing NASA's High Speed Research Program," National Academy Press, Washington, D.C., 1997.
8. Robinson, M. J., "Composite Cryogenic Propellant Tank Development," Proceedings of the 35th AIAA/ASME/ASCE/AHS/ASC Structures, Structural Dynamics and Materials Conference, Hilton Head, SC, 18-21 April 1994.
9. NASA Handbook 8060.1C (NHB 8060.1C), "Flammability, Odor, Offgassing, and Compatibility Requirements and Test Procedures for Material in Environments that Support Combustion," April 1991.
10. Robinson, M. J., Stoltzfus, J.M., Owens, T. N., "Composite Material Compatibility with Liquid Oxygen", 38th AIAA/ASME/ASCE/AHS/ASC Structures, Structural Dynamics and Materials Conference, Kissimmee, FL, 7-10 April 1997.

Acknowledgements

The authors wish to acknowledge Mr. Michael Duong, from the Boeing Company, Huntington Beach CA, Mr. Dan Reynolds from Northrop Grumman Corp., Dallas, TX, and Mr. Ken Blount from the Materials, Research and Engineering, Inc, Boulder, CO for their invaluable contributions to the test program.

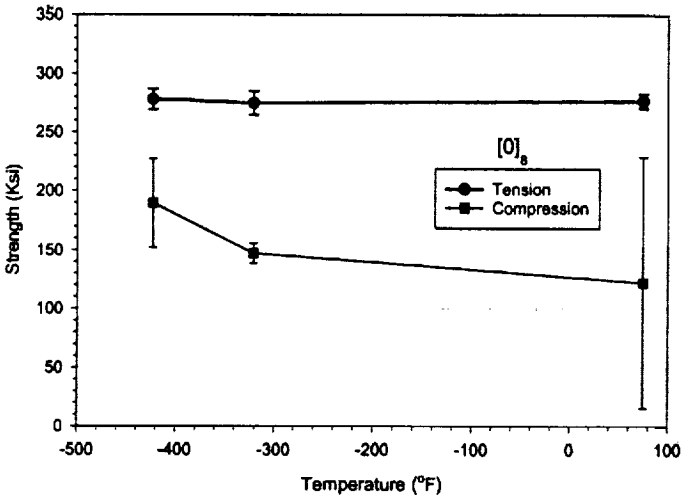

Figure 3. Effects of test temperature on unnotched strength.

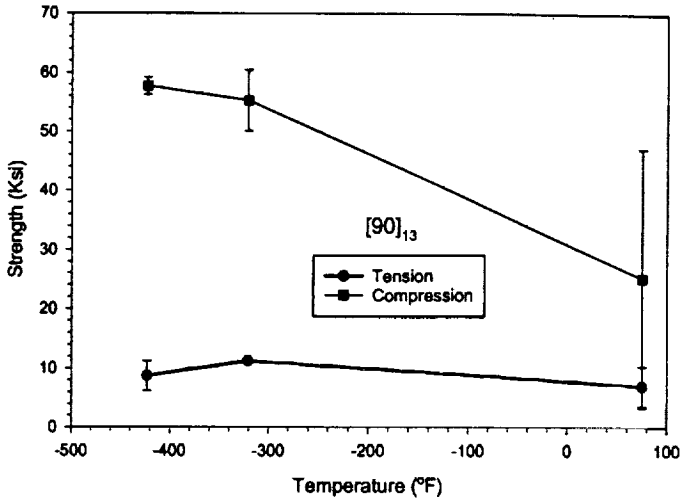

Figure 4. Effects of test temperature on unnotched strength.

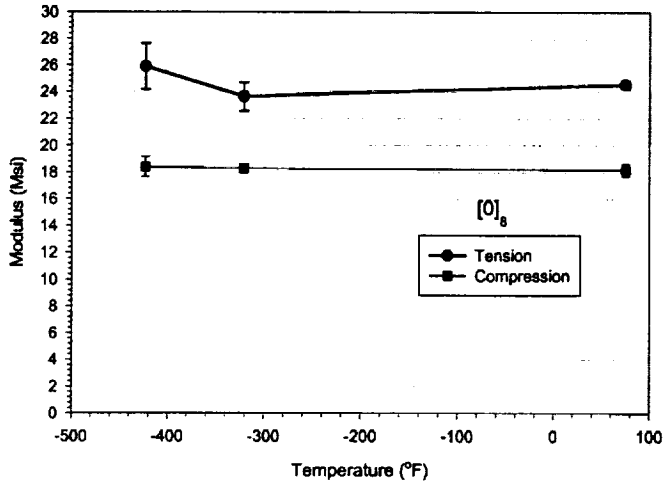

Figure 5. Effects of test temperature on unnotched longitudinal modulus.

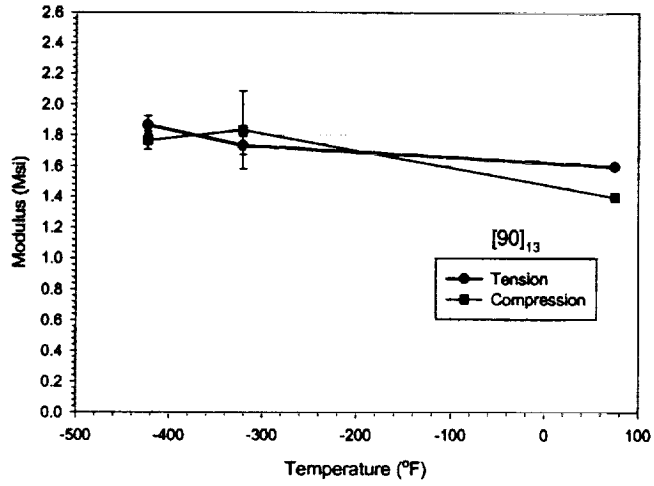

Figure 6. Effects of test temperature on unnotched transverse modulus.

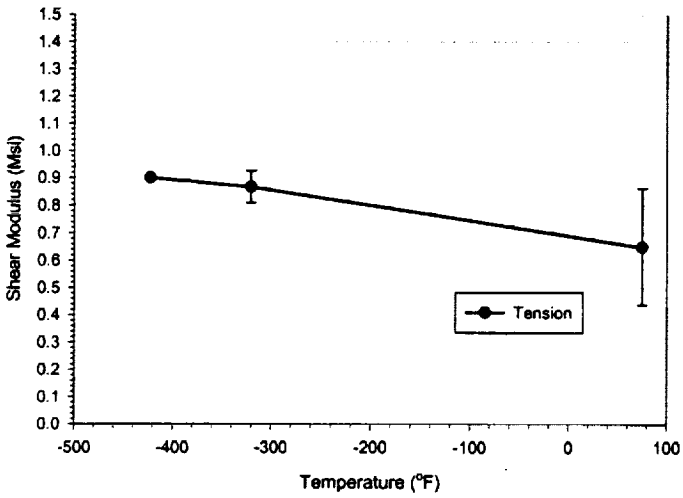

Figure 7. Effects of test temperature on unnotched shear modulus.

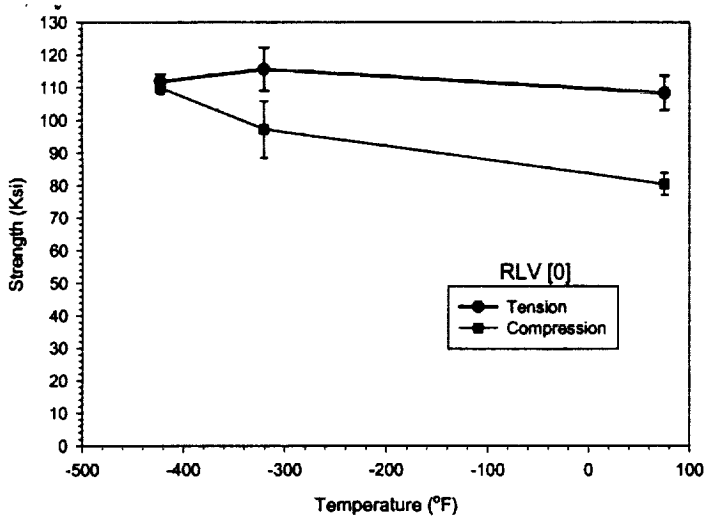

Figure 8. Effects of test temperature on unnotched strength.

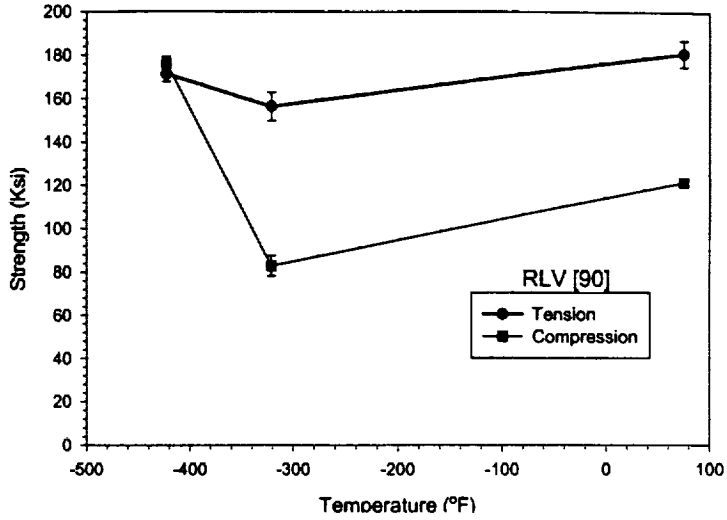

Figure 9. Effects of test temperature on unnotched strength.

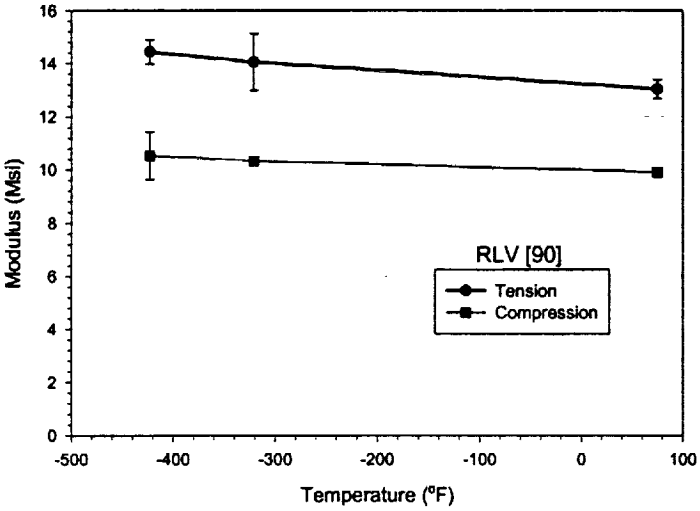

Figure 10. Effects of test temperature on unnotched longitudinal modulus.

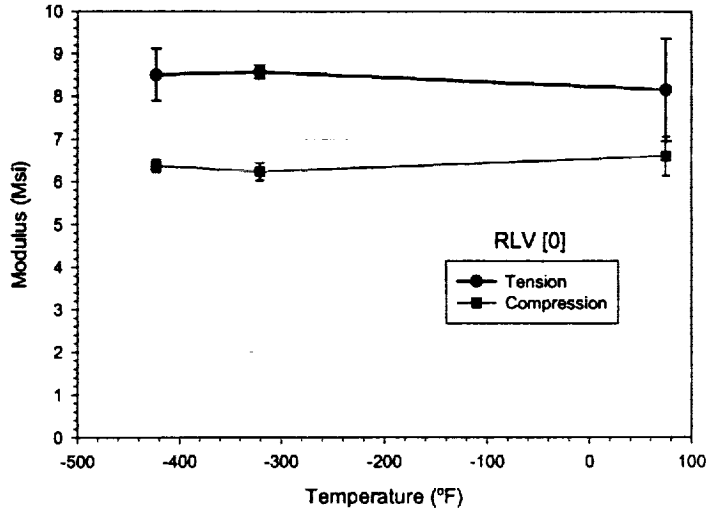

Figure 11. Effects of test temperature on unnotched transverse modulus.

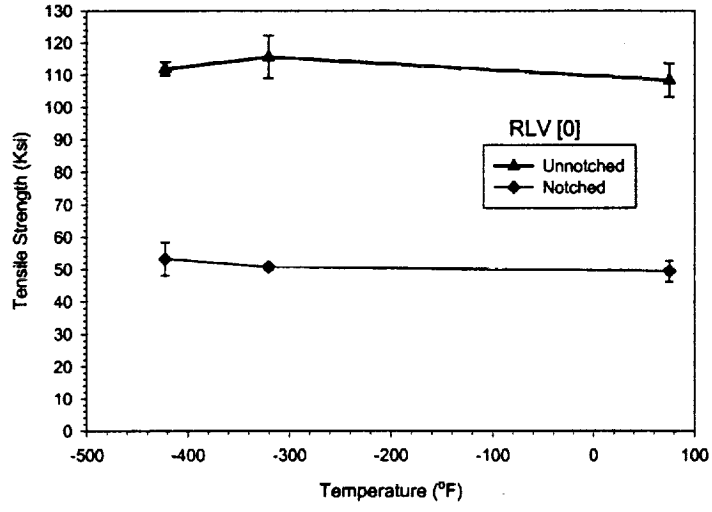

Figure 12. Effects of test temperature on longitudinal modulus.

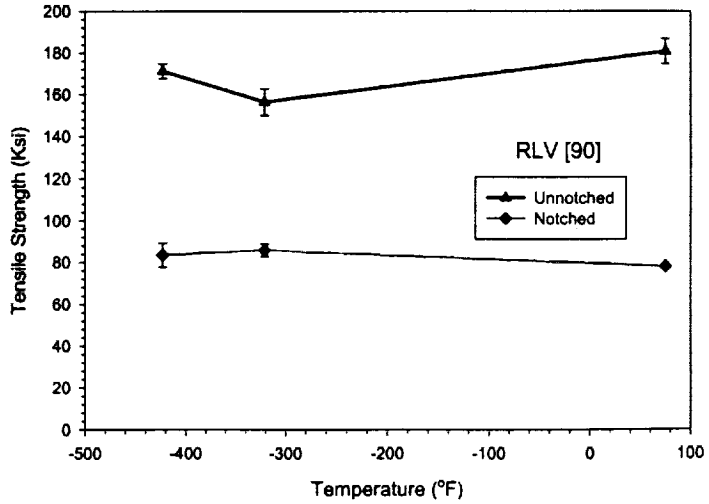

Figure 13. Effects of test temperature on transverse strength.

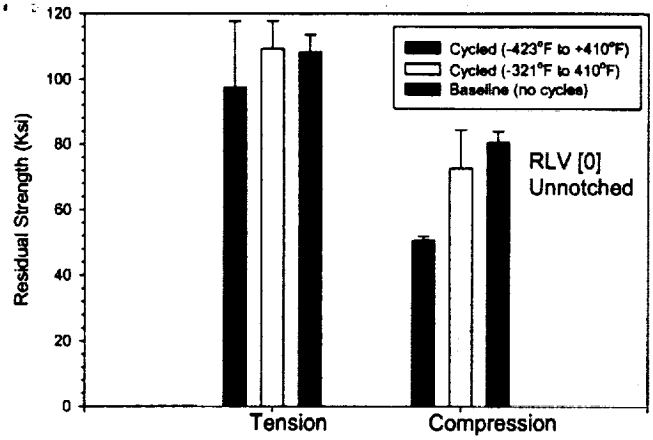

Figure 14. Effects of 35 prior thermal cycles on residual strength at room temperature.

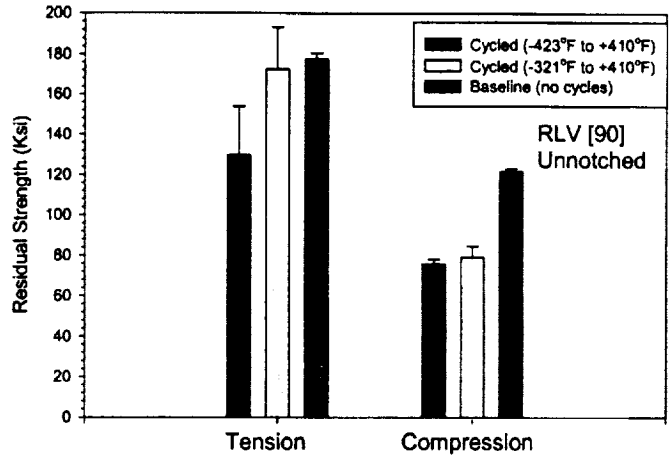

Figure 15. Effects of 35 prior thermal cycles on longitudinal residual modulus at room temperature.

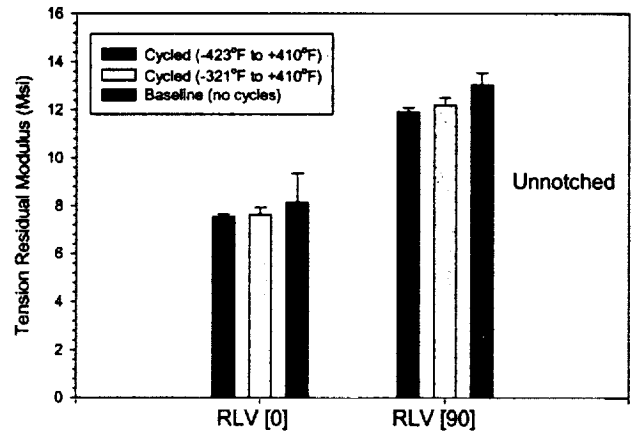

Figure 16. Effects of 35 prior thermal cycles on longitudinal and transverse residual modulus at room temperature.

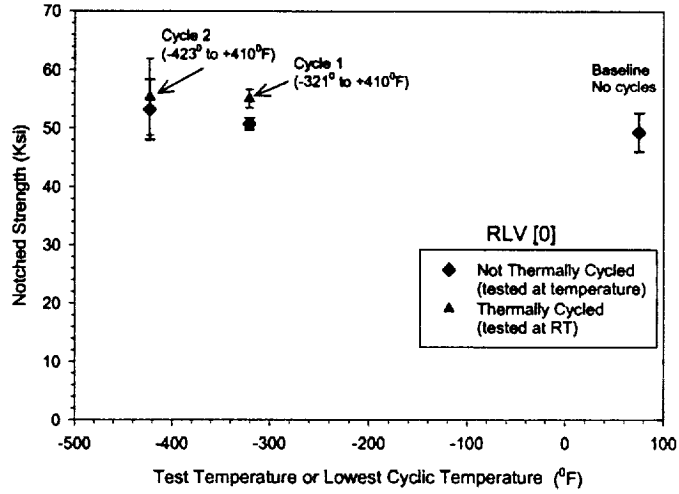

Figure 17. Effects of 35 prior thermal cycles on longitudinal notched residual strength.

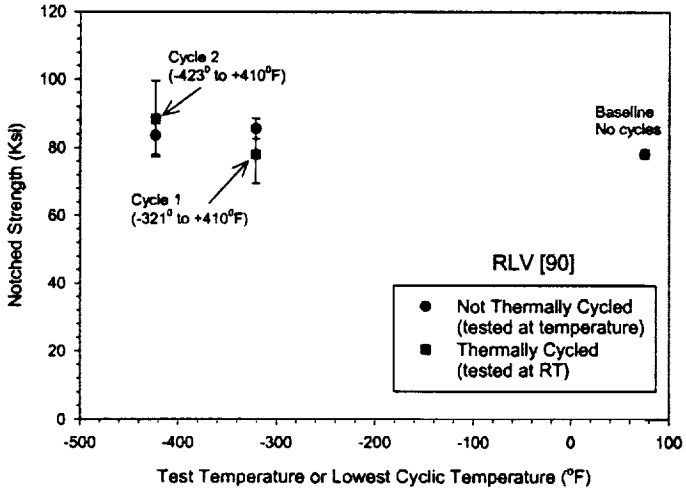

Figure 18. Effects of 35 prior thermal cycles on transverse notched residual strength.

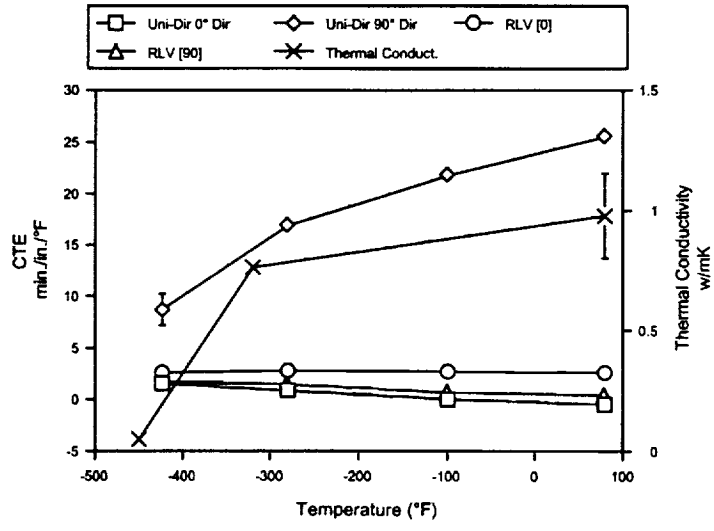

Figure 19. Coefficient of Thermal Expansion (CTE) and the through-the-thickness thermal conductivity versus temperature.